Imaging antiferromagnetic states with scanning NV-center magnetometry

Aurore Finco, Angela Haykal, Florentin Fabre, Saddem Chouaieb,
Rana Tanos, Waseem Akhtar, Vincent Jacques

Laboratoire Charles Coulomb, Université de Montpellier and CNRS, Montpellier, France

Hamburg, 24/09/2019

slides available at https://magimag.eu

How to probe non-collinear magnetism locally?

Probe directly the
sample **magnetization**

SP-STM

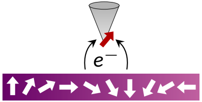

R. Wiesendanger. *Rev. Mod. Phys.* 81 (2009), 1495–1550

How to probe non-collinear magnetism locally?

Probe directly the sample **magnetization**

Probe the generated **stray field**

SP-STM

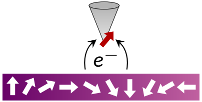

R. Wiesendanger. *Rev. Mod. Phys.* 81 (2009), 1495–1550

nano SQUIDs

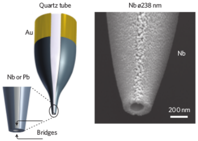

D. Vasyukov *et al.* *Nat. Nano.* 8 (2013), 639–644

Hall bars

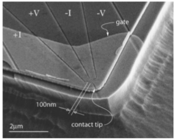

C. W. Hicks *et al.* *Appl. Phys. Lett.* 90 (2007), 133512

Single spin

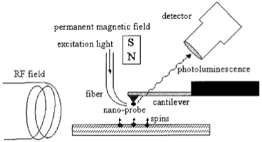

B. M. Chernobrod *et al.* *J. Appl. Phys.* 97 (2004), 014903

How to probe non-collinear magnetism locally?

Probe directly the sample **magnetization**

Probe the generated **stray field**

SP-STM

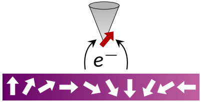

nano SQUIDs

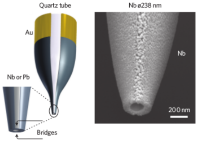

Hall bars

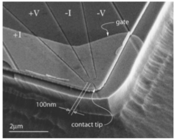

Single spin

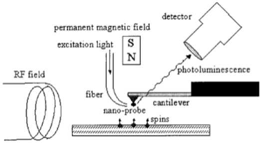

R. Wiesendanger. *Rev. Mod. Phys.* 81 (2009), 1495–1550

D. Vasyukov *et al.* *Nat. Nano.* 8 (2013), 639–644

C. W. Hicks *et al.* *Appl. Phys. Lett.* 90 (2007), 133512

B. M. Chernobrod *et al.* *J. Appl. Phys.* 97 (2004), 014903

The Nitrogen Vacancy center in diamond

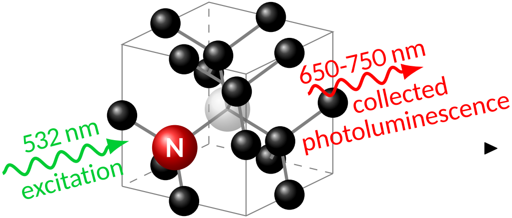

- Defect in the diamond lattice, a nitrogen atom next to a vacancy
- Artificial atom: discrete energy levels inside the diamond gap

The Nitrogen Vacancy center in diamond

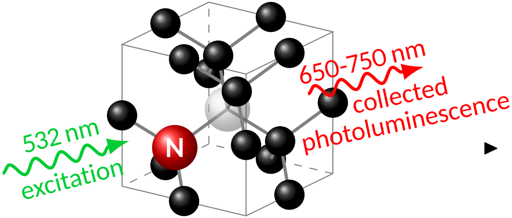

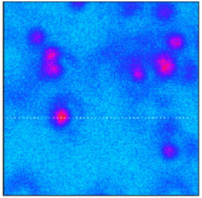

- Defect in the diamond lattice, a nitrogen atom next to a vacancy
- Artificial atom: discrete energy levels inside the diamond gap
- Stable photoluminescence at room temperature
- Single NV defects can be detected with a confocal microscope
- **Quantum magnetic field sensor**

A. Gruber *et al.* *Science* 276 (1997), 2012–2014

Scanning NV magnetometry

glued on an AFM tuning fork

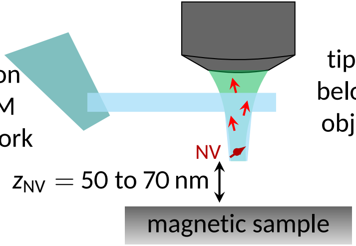

tip fixed below the objective

scanning with the sample tower

Photoluminescence scan, top view of the tip

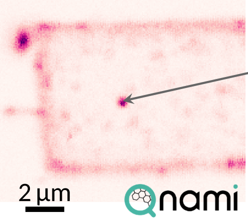

single NV

No magnetic back-action!

Scanning NV magnetometry

glued on an AFM tuning fork

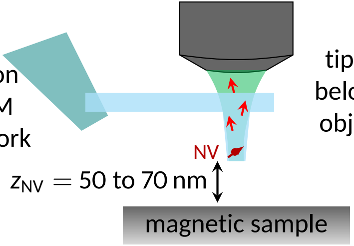

tip fixed below the objective

scanning with the sample tower

Photoluminescence scan, top view of the tip

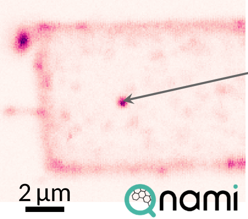

single NV

No magnetic back-action!

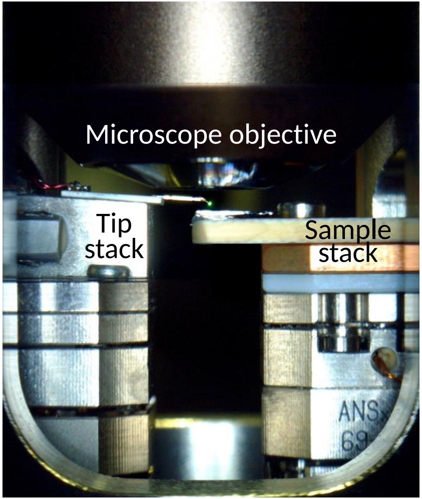

Quantitative field measurements

Spin-dependent fluorescence

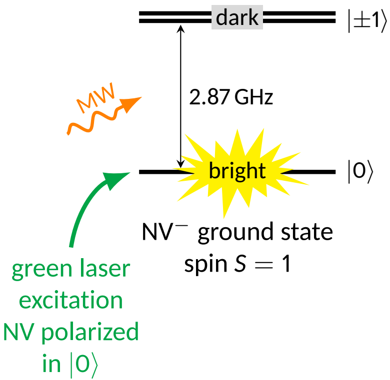

Quantitative field measurements

Spin-dependent fluorescence

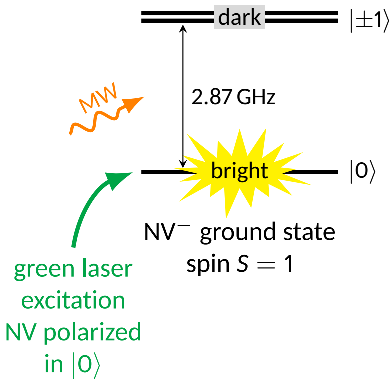

Optically Detected Magnetic Resonance

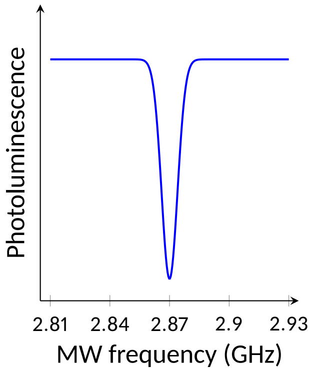

Quantitative field measurements

Spin-dependent fluorescence

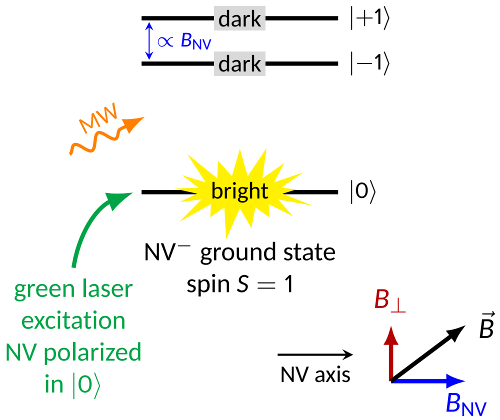

Optically Detected Magnetic Resonance

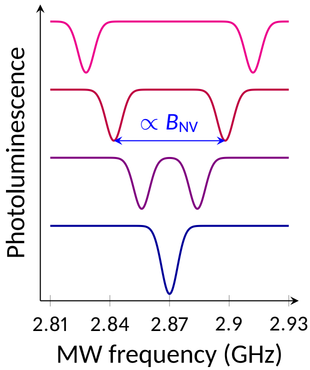

Quenching of the photoluminescence at high field

Mixing of the spin states

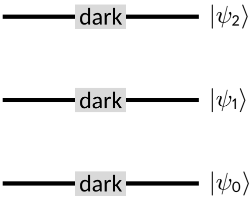

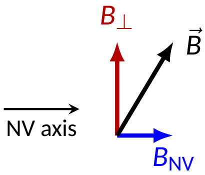

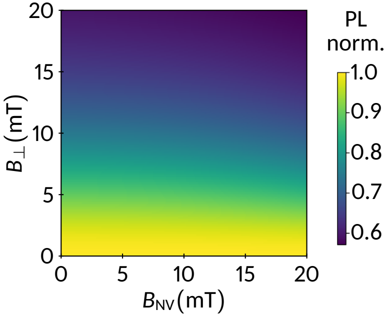

J.-P. Tetienne *et al.* *New J. Phys.* 14 (2012), 103033

Two measurement modes

Quantitative mode

Low field regime ($B_\perp < 5\,\mathrm{mT}$)

- Gives access to the precise value of the stray field along the NV axis, sensitivity $1\,\mu\mathrm{T\,Hz}^{-1/2}$
- Need to measure a spectrum at each pixel to localize the resonance
- Requires a microwave excitation
- Slow, sensitive to drift

Investigation of antiferromagnets

Two measurement modes

Quantitative mode

Low field regime ($B_\perp < 5$ mT)

- Gives access to the precise value of the stray field along the NV axis, sensitivity $1\,\mu\mathrm{T\,Hz}^{-1/2}$
- Need to measure a spectrum at each pixel to localize the resonance
- Requires a microwave excitation
- Slow, sensitive to drift

Investigation of antiferromagnets

Qualitative mode

High field regime ($B_\perp > 5$ mT)

- Localize the areas producing a large stray field
- Only need to record the photoluminescence at each pixel
- No microwave excitation required
- Strength of the measured field unknown

Study of ferromagnets

Zero-field skyrmions in exchange-biased magnetic layers

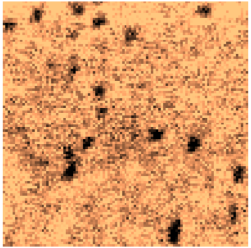

Collaboration

O. Boulle group, Grenoble

Influence of epitaxial strain on the cycloid in the multiferroic $BiFeO_3$

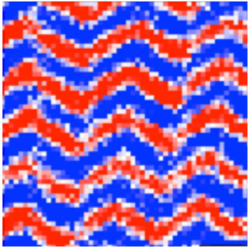

Collaboration

S. Fusil and V. Garcia group
M. Viret group, Palaiseau

Detection of domain wall magnons in a synthetic antiferromagnet

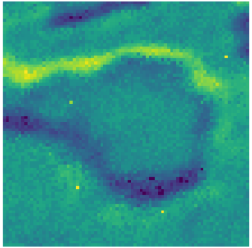

Collaboration

V. Cros group
J.-V. Kim, Palaiseau

Zero-field skyrmions in exchange-biased magnetic layers

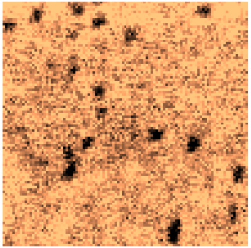

Collaboration

spintec SPIN IN ELECTRONICS

O. Boulle group, Grenoble

Influence of epitaxial strain on the cycloid in the multiferroic $BiFeO_3$

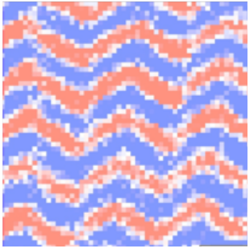

Collaboration

cnrs THALES cea

S. Fusil and V. Garcia group
M. Viret group, Palaiseau

Detection of domain wall magnons in a synthetic antiferromagnet

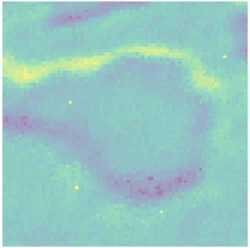

Collaboration

cnrs THALES C2N

V. Cros group
J.-V. Kim, Palaiseau

Use exchange bias as an effective field

Goal: stable zero-field skyrmions at room temperature without confinement

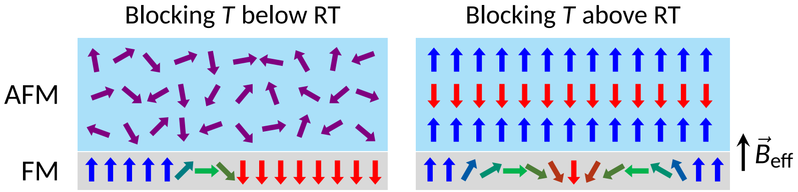

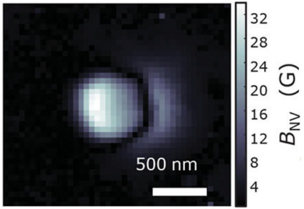

IrMn/CoFeB stack
µm-sized skyrmions

G. Yu *et al.* *Nano Lett.* 18 (2018), 980–986

Use exchange bias as an effective field

Goal: stable zero-field skyrmions at room temperature without confinement

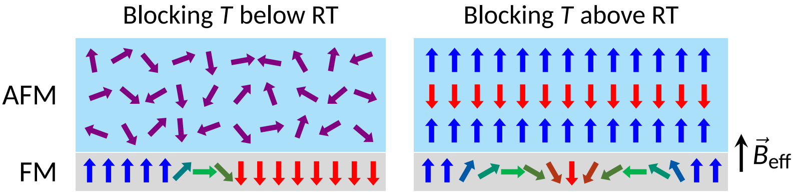

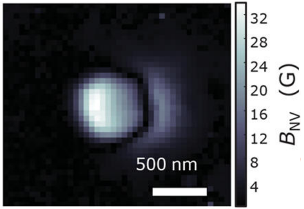

IrMn/CoFeB stack
µm-sized skyrmions

G. Yu *et al.* *Nano Lett.* 18 (2018), 980–986

Strategy to reduce the skyrmion size

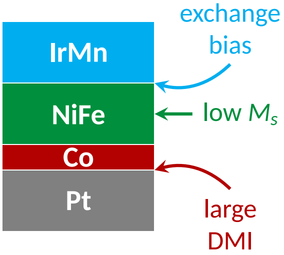

O. Boulle, G. Rana
L. Buda-Prejbeanu

spintec

Optimization of the sample parameters

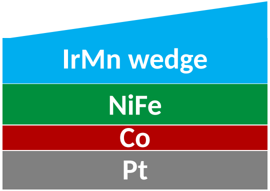

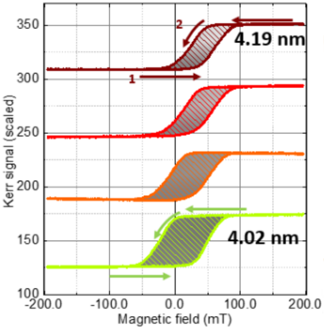

$t_{\mathrm{IrMn}} = 4.02\,\mathrm{nm}$ $t_{\mathrm{IrMn}} = 4.11\,\mathrm{nm}$ $t_{\mathrm{IrMn}} = 4.15\,\mathrm{nm}$ $t_{\mathrm{IrMn}} = 4.19\,\mathrm{nm}$

MFM images

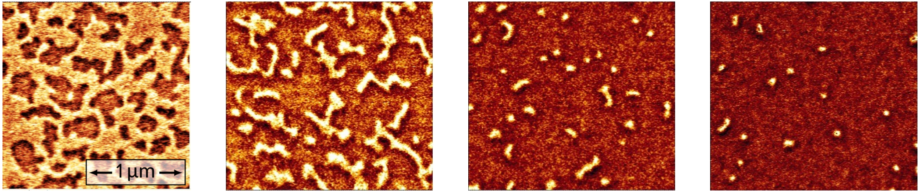

Magnetic skyrmions in qualitative “quenching” mode

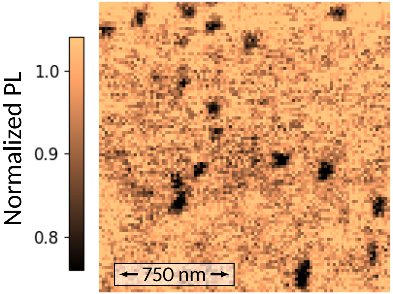

Magnetic skyrmions in qualitative “quenching” mode

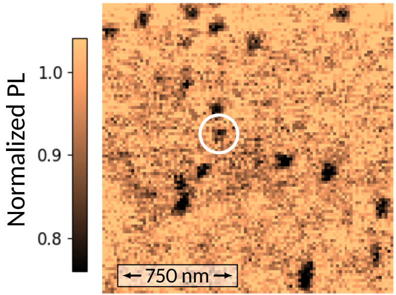

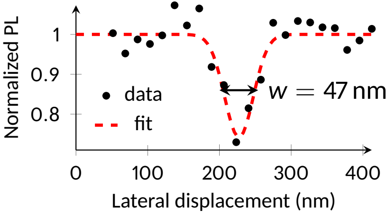

Magnetic skyrmions in qualitative “quenching” mode

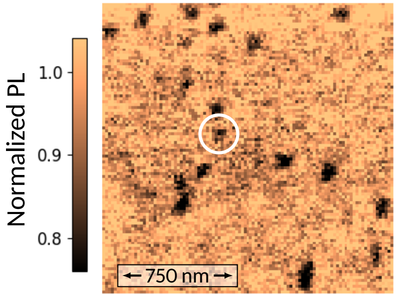

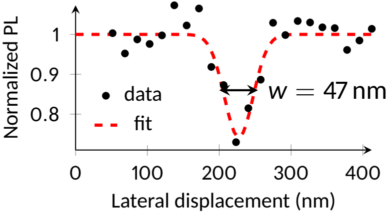

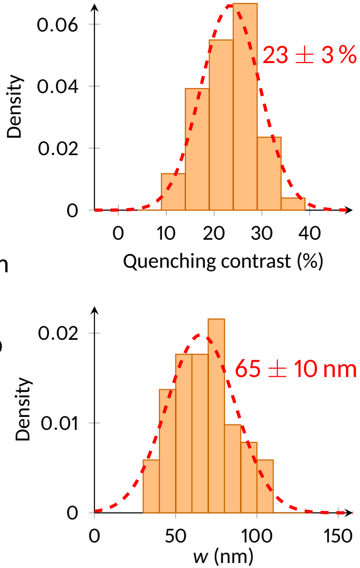

Comparison with simulations

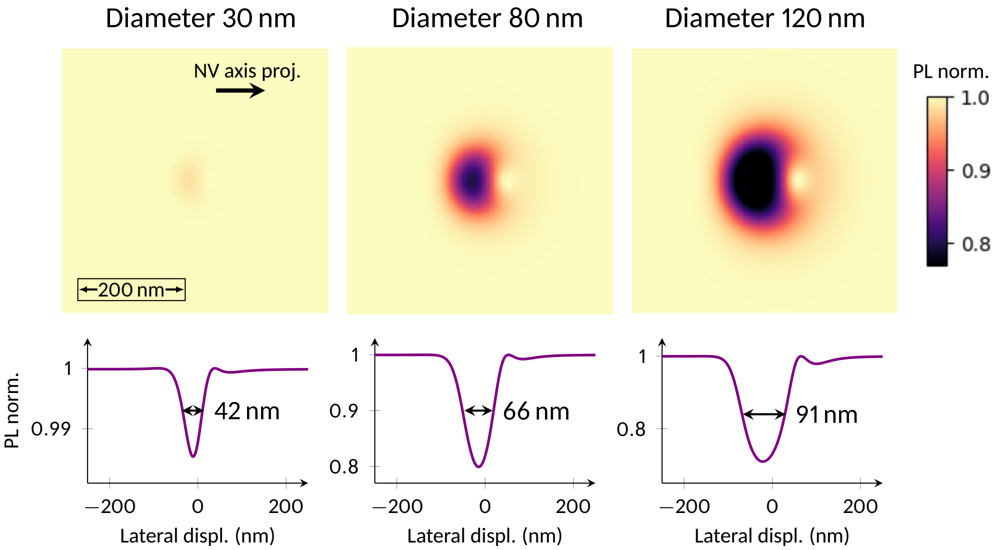

Zero-field skyrmions in exchange-biased magnetic layers

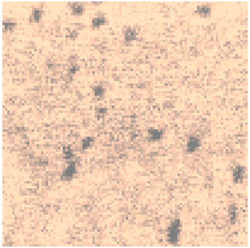

Collaboration

O. Boulle group, Grenoble

Influence of epitaxial strain on the cycloid in the multiferroic $BiFeO_3$

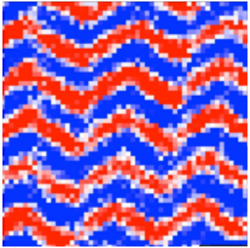

Collaboration

S. Fusil and V. Garcia group
M. Viret group, Palaiseau

Detection of domain wall magnons in a synthetic antiferromagnet

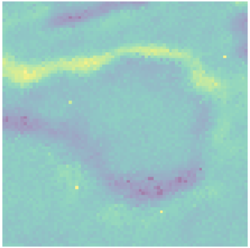

Collaboration

V. Cros group
J.-V. Kim, Palaiseau

How to control the spin state of antiferromagnets?

With magnetic field? No, antiferromagnets are insensitive to external fields!

With current?

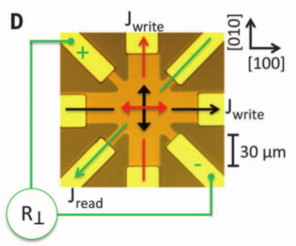

P. Wadley *et al.* *Science* 351 (2016), 587–590

With strain?

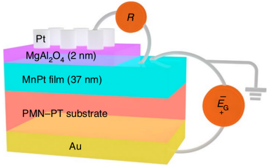

H. Yan *et al.* *Nat. Nano.* 14 (2019), 131

Here: apply strain on a multiferroic to combine strain and magnetoelectric effects

$BiFeO_3$, a room temperature multiferroic

Electric polarization

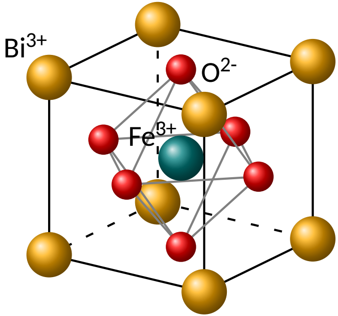

Paraelectric phase (T>1100 K)

G. Catalan *et al.* *Adv. Mater.* 21 (2009), 2463–2485

$BiFeO_3$, a room temperature multiferroic

Electric polarization

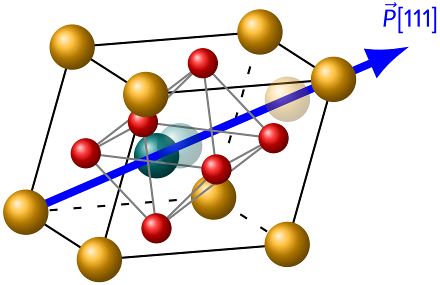

Ferroelectric phase (T<1100 K)

G. Catalan *et al.* *Adv. Mater.* 21 (2009), 2463–2485

$BiFeO_3$, a room temperature multiferroic

Electric polarization

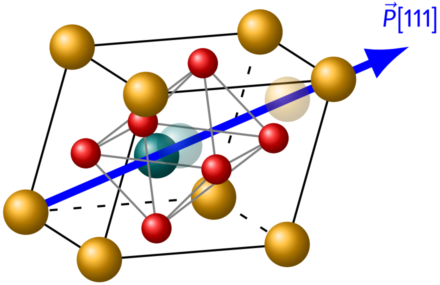

Magnetism

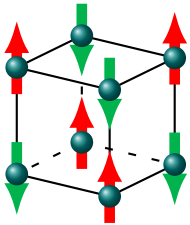

G-type
antiferromagnet

Ferroelectric phase (T<1100 K)

G. Catalan *et al.* *Adv. Mater.* 21 (2009), 2463–2485

$BiFeO_3$, a room temperature multiferroic

Electric polarization

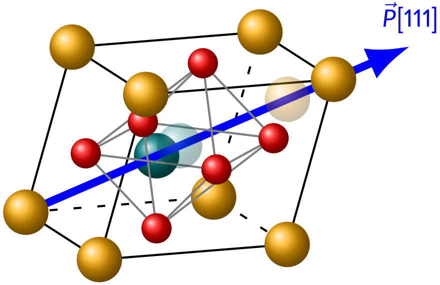

Ferroelectric phase (T<1100 K)

Magnetism

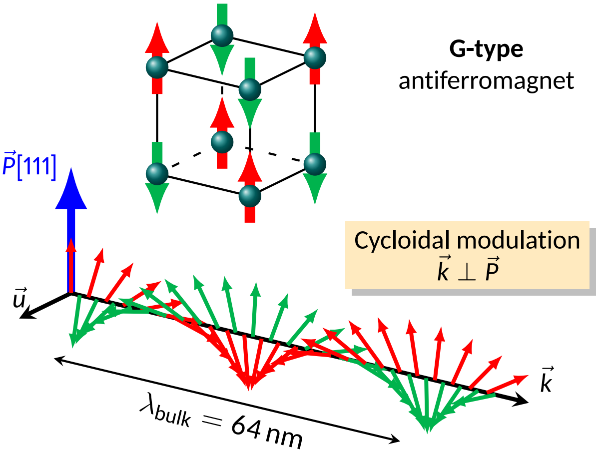

G. Catalan *et al.* *Adv. Mater.* 21 (2009), 2463–2485

Origin of the stray field: spin density wave

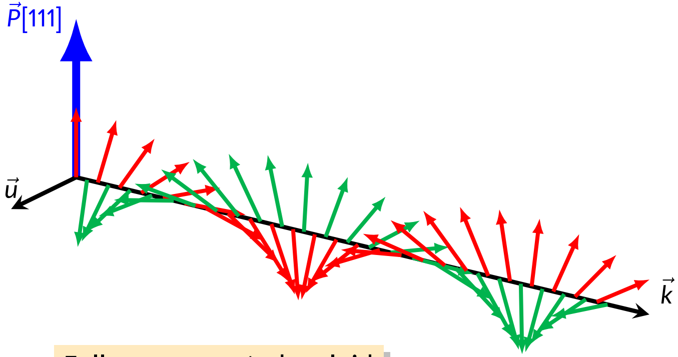

Fully compensated cycloid
→ **No stray field!**

Origin of the stray field: spin density wave

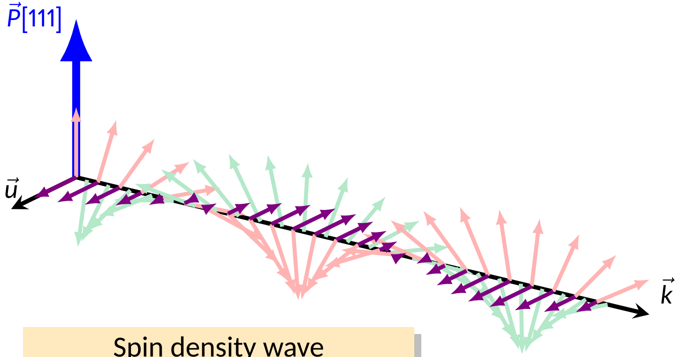

Spin density wave
Weak uncompensated moment
→ **Small stray field**

M. Ramazanoglu *et al.* *Phys. Rev. Lett.* 107 (2011), 207206

Origin of the stray field: spin density wave

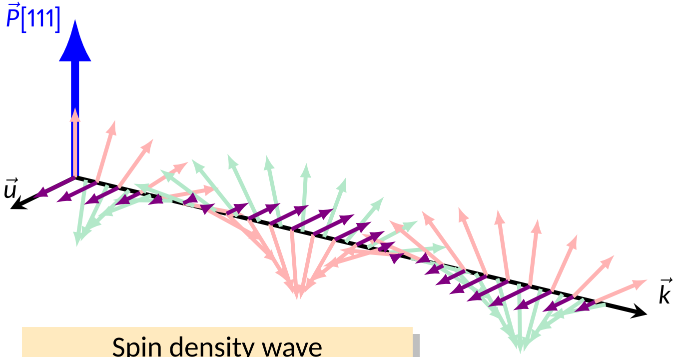

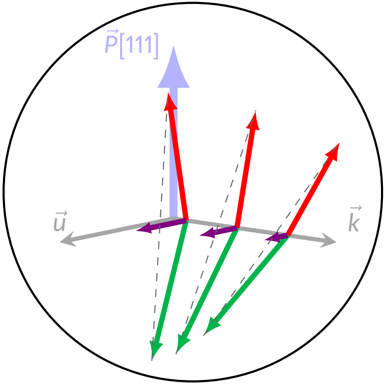

Spin density wave
Weak uncompensated moment
→ **Small stray field**

M. Ramazanoglu *et al.* *Phys. Rev. Lett.* 107 (2011), 207206

Known effect of epitaxial strain on the cycloid

Phase diagram obtained from spectroscopic measurements

Epitaxial strain tuned by changing the substrate

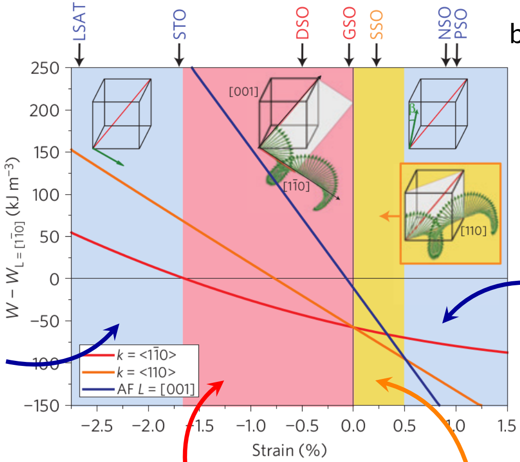

Large tensile strain
antiferromagnetic order

Large compressive strain
antiferromagnetic order

Small compressive strain
cycloid type I

Small tensile strain
cycloid type II

D. Sando *et al*. *Nat. Mater.* 12 (2013), 641–646

Tuning of epitaxial strain

$BiFeO_3$ thin film samples grown on various substrates

Samples from UMR CNRS/Thales
J. Fischer, V. Garcia, S. Fusil

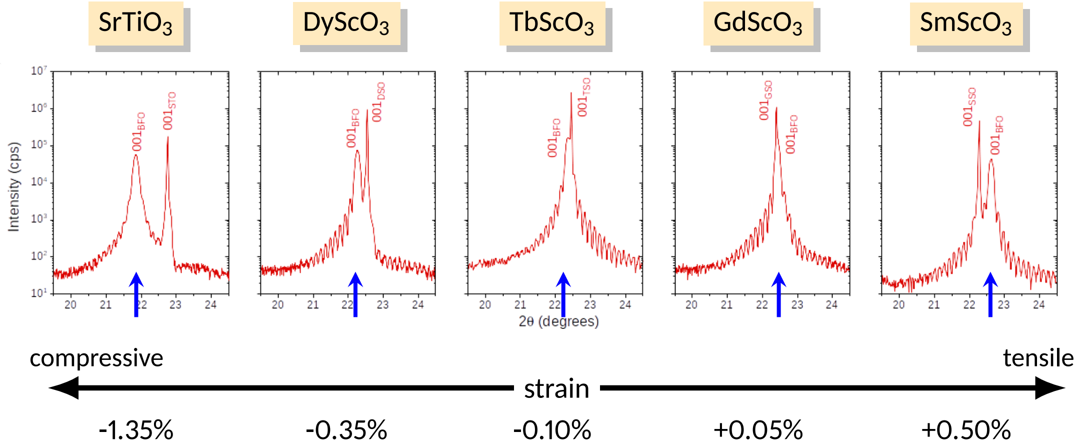

NV imaging of the cycloid, iso-B mode

$DyScO_3$, strain -0.35%

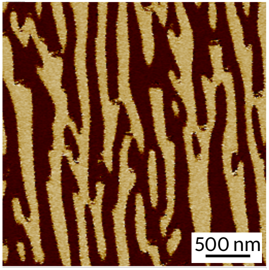

PFM image
ferroelectric domains

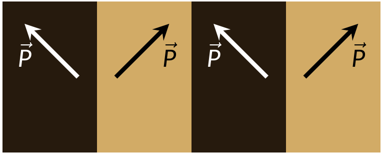

I. Gross *et al.* *Nature* 549 (2017), 252–256

NV imaging of the cycloid, iso-B mode

$DyScO_3$, strain -0.35%

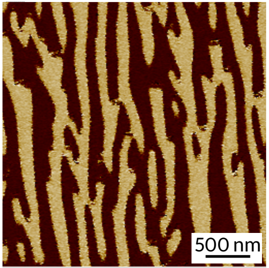

PFM image
ferroelectric domains

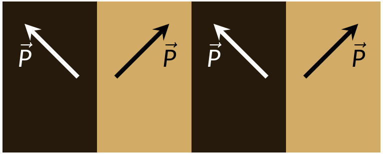

Reference spectrum
resonance shifted by
a permanent magnet

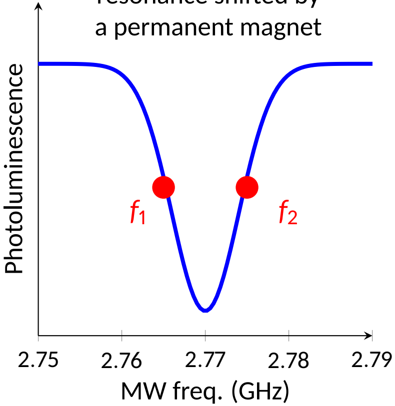

$$\Delta PL = PL(f_2) - PL(f_1)$$

I. Gross *et al.* *Nature* 549 (2017), 252–256

NV imaging of the cycloid, iso-B mode

$DyScO_3$, strain -0.35%

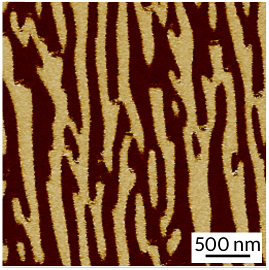

PFM image
ferroelectric domains

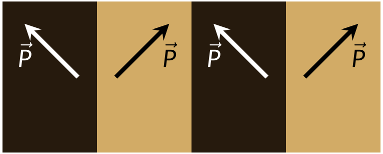

Spectrum for

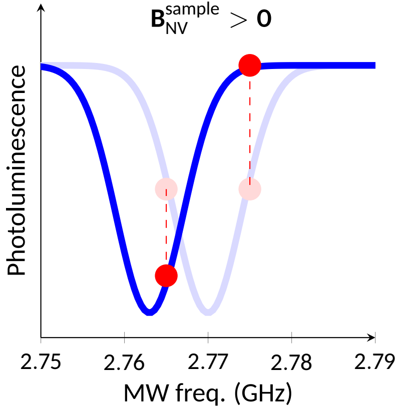

$$\Delta PL = PL(f_2) - PL(f_1)$$

$$\Delta PL > 0$$

I. Gross *et al.* *Nature* 549 (2017), 252–256

NV imaging of the cycloid, iso-B mode

$DyScO_3$, strain -0.35%

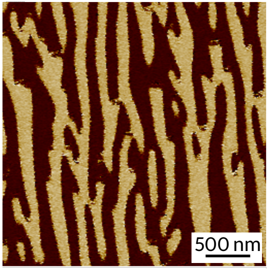

PFM image
ferroelectric domains

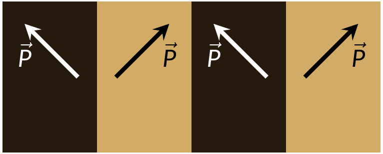

Spectrum for

$\mathbf{B}_{\mathrm{NV}}^{\mathrm{sample}} < \mathbf{0}$

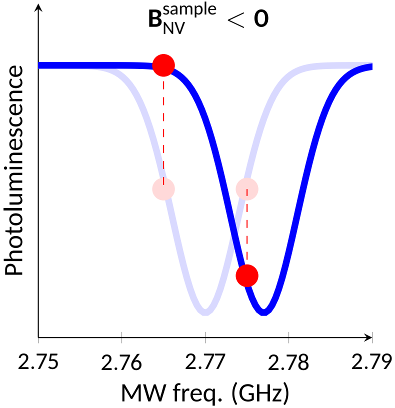

$$\Delta \mathrm{PL} = \mathrm{PL}(f_2) - \mathrm{PL}(f_1)$$

$$\Delta \mathrm{PL} < 0$$

I. Gross *et al.* *Nature* 549 (2017), 252–256

NV imaging of the cycloid, iso-B mode

$DyScO_3$, strain -0.35%

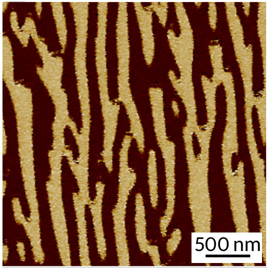

PFM image
ferroelectric domains

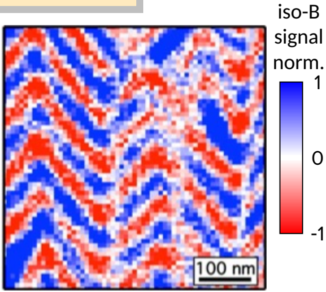

NV image
cycloid

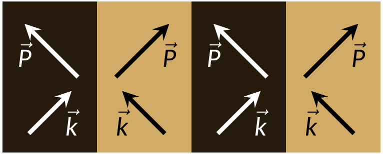

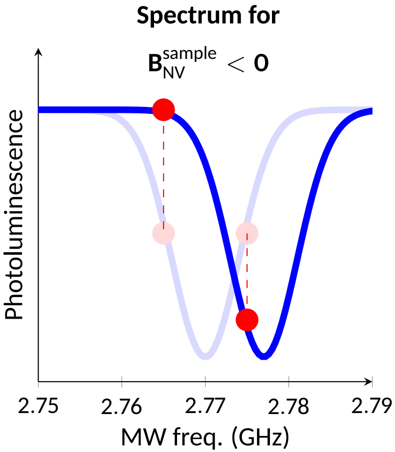

$$\Delta\mathrm{PL} = \mathrm{PL}(f_2) - \mathrm{PL}(f_1)$$

$$\Delta\mathrm{PL} < 0$$

I. Gross *et al.* *Nature* 549 (2017), 252–256

NV imaging of the cycloid, iso-B mode

$DyScO_3$, strain -0.35%

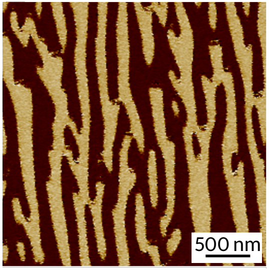

PFM image
ferroelectric domains

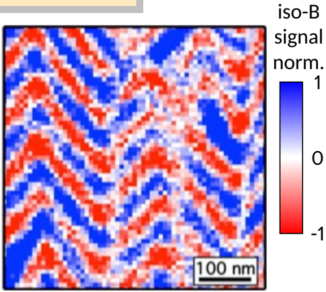

NV image
cycloid

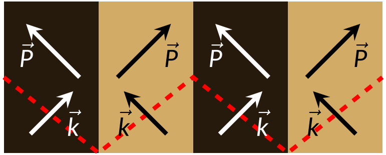

Spectrum for

$\mathbf{B}_{\mathrm{NV}}^{\mathrm{sample}} < \mathbf{0}$

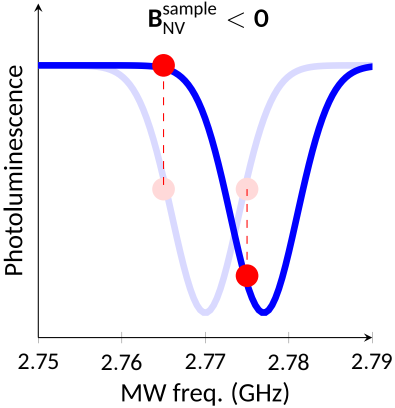

$$\Delta \mathrm{PL} = \mathrm{PL}(f_2) - \mathrm{PL}(f_1)$$

$$\Delta \mathrm{PL} < 0$$

I. Gross *et al.* *Nature* 549 (2017), 252–256

The type I cycloid

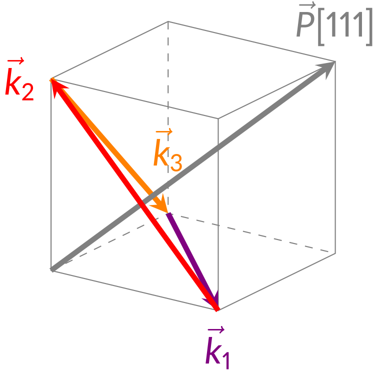

$\vec{k}_1 \parallel [1\bar{1}0]$
$\vec{k}_2 \parallel [\bar{1}01]$
$\vec{k}_3 \parallel [01\bar{1}]$

The type I cycloid

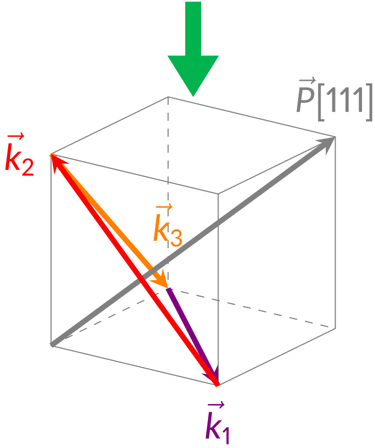

$\vec{k}_1 \parallel [1\bar{1}0]$
$\vec{k}_2 \parallel [\bar{1}01]$
$\vec{k}_3 \parallel [01\bar{1}]$

Top view

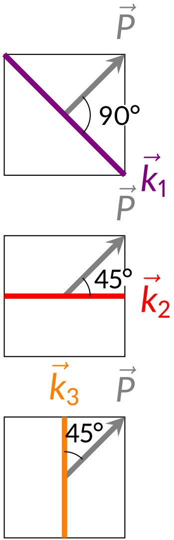

$\lambda_{\mathrm{IP}} = \lambda_{\mathrm{bulk}}$
64 nm

$\lambda_{\mathrm{IP}} = \sqrt{2}\lambda_{\mathrm{bulk}}$
90 nm

$\lambda_{\mathrm{IP}} = \sqrt{2}\lambda_{\mathrm{bulk}}$
90 nm

Stripy ferroelectric domains

$DyScO_3$

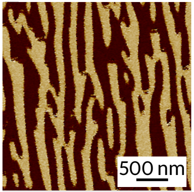

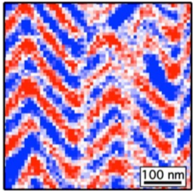

-0.35%

compressive ← strain → tensile

type I cycloid

$\vec{k}_1$

Stripy ferroelectric domains

$DyScO_3$

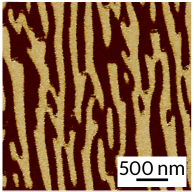

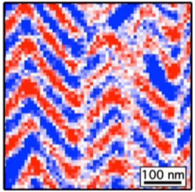

-0.35%

$GdScO_3$

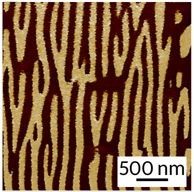

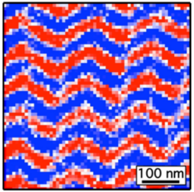

+0.05%

compressive ← strain → tensile

type I cycloid

$\vec{k}_1$

type II cycloid?

The type II cycloid

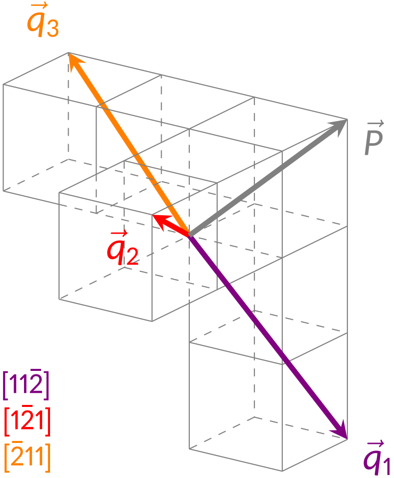

$\vec{q}_1 \parallel [11\bar{2}]$
$\vec{q}_2 \parallel [1\bar{2}1]$
$\vec{q}_3 \parallel [\bar{2}11]$

D. Sando *et al.* *Nat. Mater.* 12 (2013), 641–646

The type II cycloid

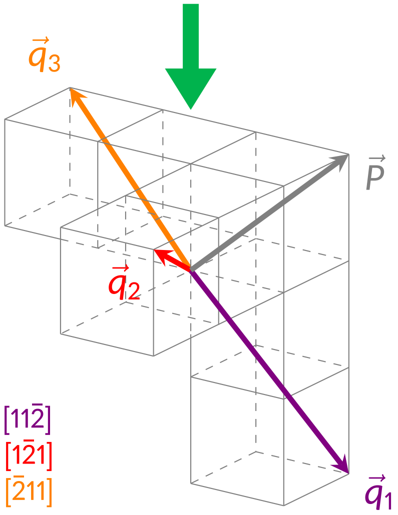

$\vec{q}_1 \parallel [11\bar{2}]$
$\vec{q}_2 \parallel [1\bar{2}1]$
$\vec{q}_3 \parallel [\bar{2}11]$

Top view

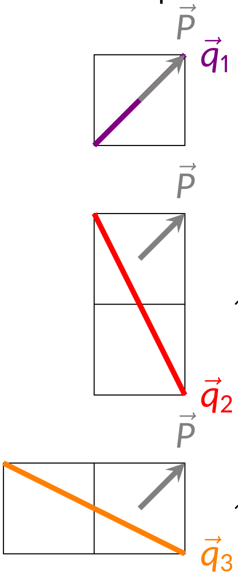

$\lambda_{\mathrm{IP}} = \sqrt{3}\lambda_{\mathrm{bulk}}$
111 nm

$\lambda_{\mathrm{IP}} = \sqrt{\frac{6}{5}}\lambda_{\mathrm{bulk}}$
70 nm

$\lambda_{\mathrm{IP}} = \sqrt{\frac{6}{5}}\lambda_{\mathrm{bulk}}$
70 nm

D. Sando *et al.* *Nat. Mater.* 12 (2013), 641–646

The type II cycloid

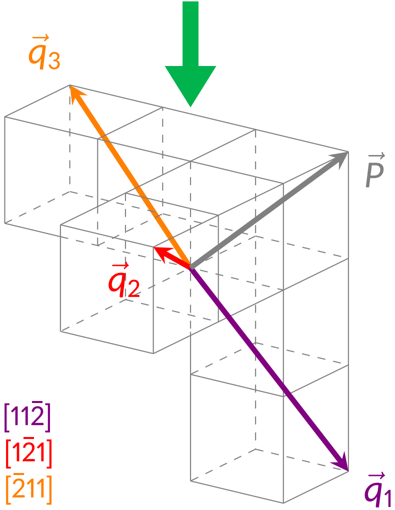

$\vec{q}_1 \parallel [11\bar{2}]$
$\vec{q}_2 \parallel [1\bar{2}1]$
$\vec{q}_3 \parallel [\bar{2}11]$

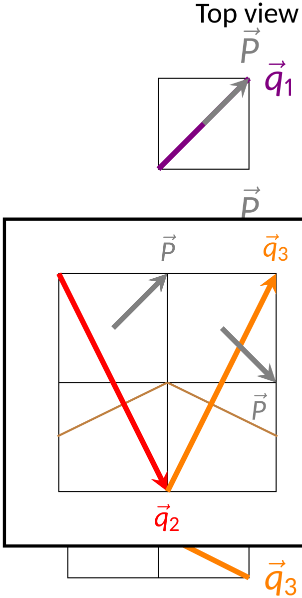

$\lambda_{\text{IP}} = \sqrt{3}\lambda_{\text{bulk}}$
111 nm

$= \sqrt{\frac{6}{5}}\lambda_{\text{bulk}}$
70 nm

$= \sqrt{\frac{6}{5}}\lambda_{\text{bulk}}$
70 nm

D. Sando *et al.* *Nat. Mater.* 12 (2013), 641–646

X-ray diffraction

N. Jaouen, J.-Y. Chauleau, M. Viret

$DyScO_3$

type I cycloid

$\vec{k}_1$

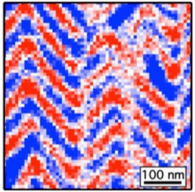

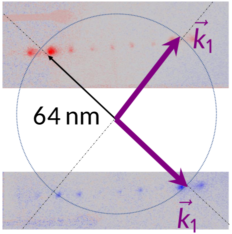

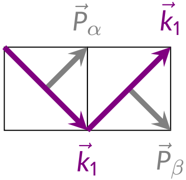

$\lambda_{\text{IP}} = \lambda_{\text{bulk}}$

64 nm

X-ray diffraction

N. Jaouen, J.-Y. Chauleau, M. Viret

$DyScO_3$

type I cycloid

$\vec{k}_1$

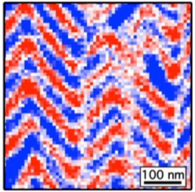

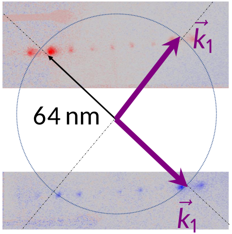

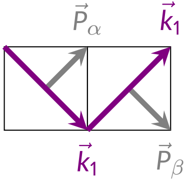

$$\lambda_{\text{IP}} = \lambda_{\text{bulk}}$$

64 nm

$GdScO_3$

type II cycloid

$\vec{q}_2, \vec{q}_3$

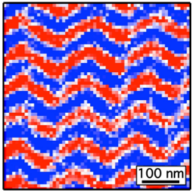

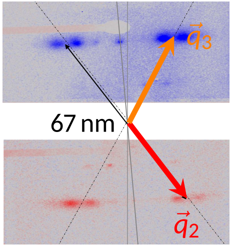

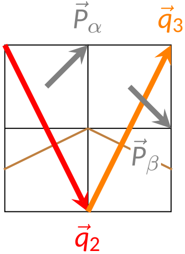

$$\lambda_{\text{IP}} = \sqrt{\frac{6}{5}}\lambda_{\text{bulk}}$$

70 nm

Stripy ferroelectric domains

$DyScO_3$

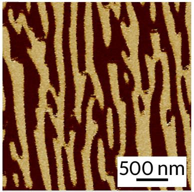

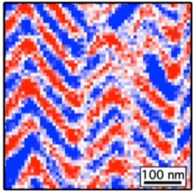

-0.35%

$GdScO_3$

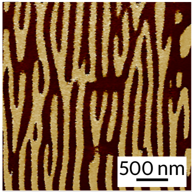

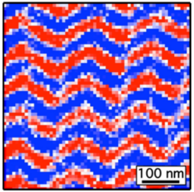

+0.05%

compressive ⟵ strain ⟶ tensile

type I cycloid

$\vec{k}_1$

type II cycloid

$\vec{q}_2, \vec{q}_3$

Stripy ferroelectric domains

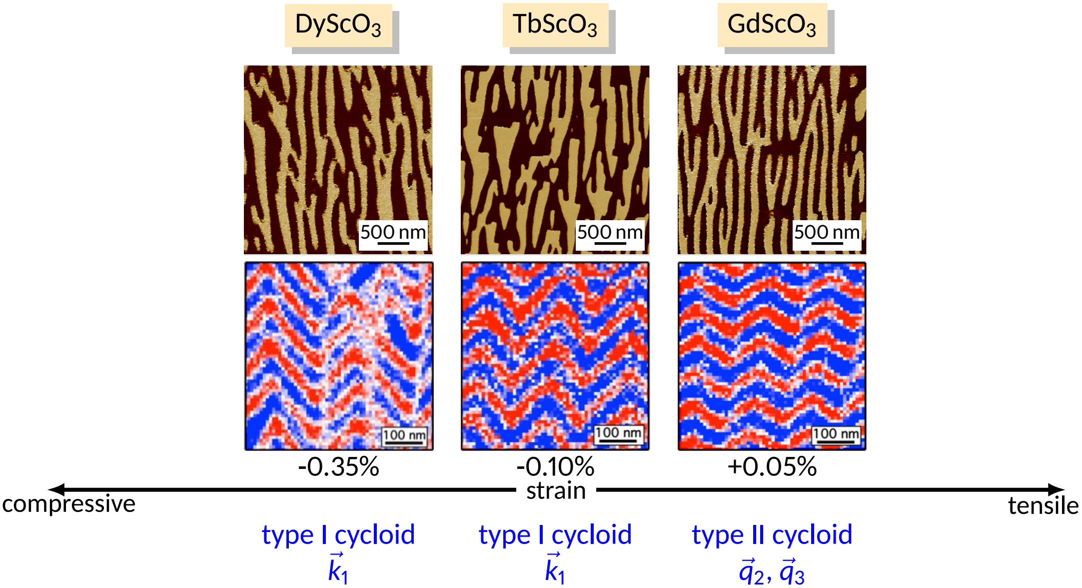

Stripy ferroelectric domains

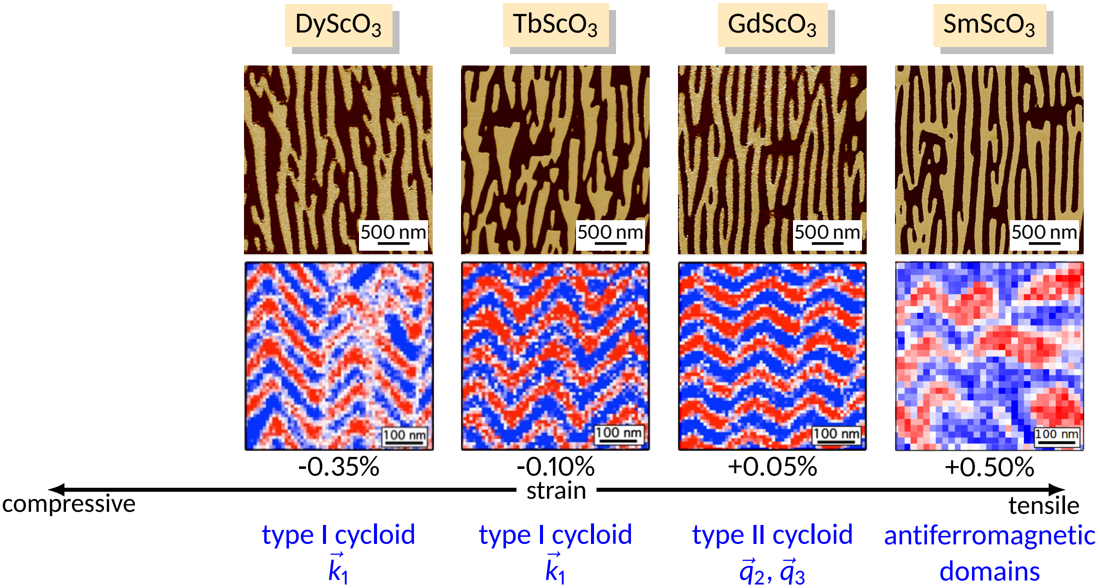

Stripy ferroelectric domains

SrTiO$_3$ | DyScO$_3$ | TbScO$_3$ | GdScO$_3$ | SmScO$_3$

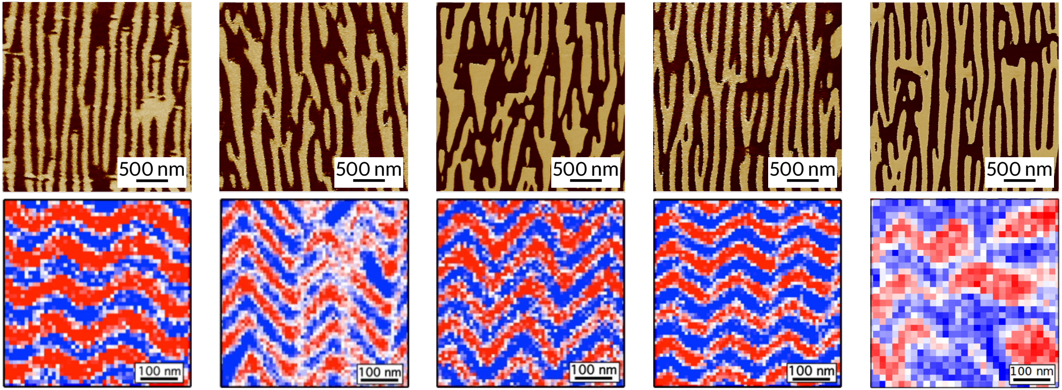

-1.35% | -0.35% | -0.10% | +0.05% | +0.50%

compressive ← strain → tensile

type II cycloid $\vec{q}_2, \vec{q}_3$ | type I cycloid $\vec{k}_1$ | type I cycloid $\vec{k}_1$ | type II cycloid $\vec{q}_2, \vec{q}_3$ | antiferromagnetic domains

Known effect of epitaxial strain on the cycloid

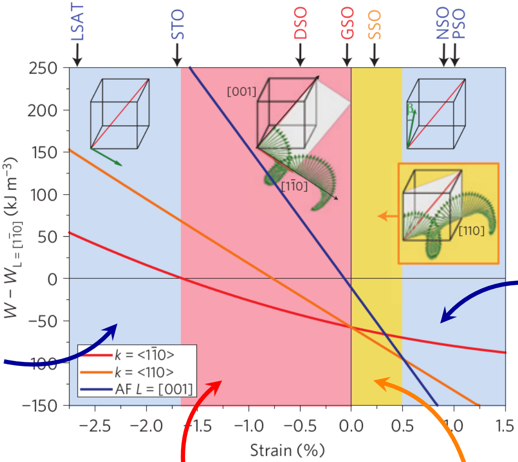

Large tensile strain
antiferromagnetic order

Large compressive strain
antiferromagnetic order

Small compressive strain
cycloid type I

Small tensile strain
cycloid type II

D. Sando *et al.* *Nat. Mater.* 12 (2013), 641–646

Manipulation via magnetoelectric coupling

PFM image	$DyScO_3$	$TbScO_3$	$GdScO_3$	$SmScO_3$
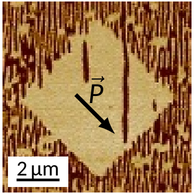	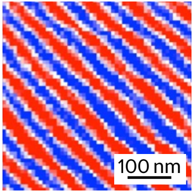	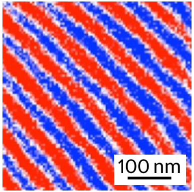	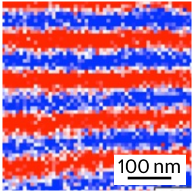	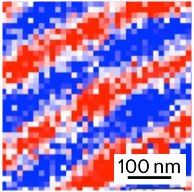
	$\lambda_{\mathrm{IP}}^{\mathrm{meas}} = 68\,\mathrm{nm}$	$\lambda_{\mathrm{IP}}^{\mathrm{meas}} = 67\,\mathrm{nm}$	$\lambda_{\mathrm{IP}}^{\mathrm{meas}} = 92\,\mathrm{nm}$	$\lambda_{\mathrm{IP}}^{\mathrm{meas}} = 130\,\mathrm{nm}$
	-0.35%	-0.10%	+0.05%	+0.50%

← strain →

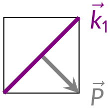	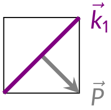	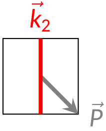	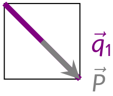
$\lambda_{\mathrm{IP}}^{\mathrm{th}} = 64\,\mathrm{nm}$	$\lambda_{\mathrm{IP}}^{\mathrm{th}} = 64\,\mathrm{nm}$	$\lambda_{\mathrm{IP}}^{\mathrm{th}} = 90\,\mathrm{nm}$	$\lambda_{\mathrm{IP}}^{\mathrm{th}} = 111\,\mathrm{nm}$
type I cycloid $\vec{k}_1$	type I cycloid $\vec{k}_1$	type I cycloid $\vec{k}_2$	type II cycloid $\vec{q}_1$

Zero-field skyrmions in exchange-biased magnetic layers	Influence of epitaxial strain on the cycloid in the multiferroic $BiFeO_3$	**Detection of domain wall magnons in a synthetic antiferromagnet**
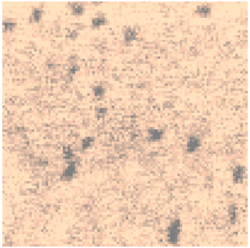	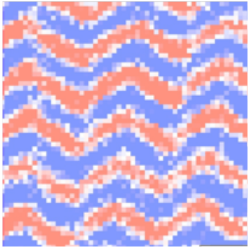	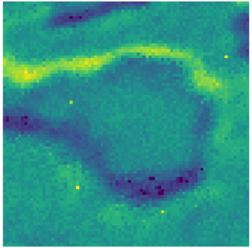
Collaboration	Collaboration	Collaboration
O. Boulle group, Grenoble	S. Fusil and V. Garcia group M. Viret group, Palaiseau	V. Cros group J.-V. Kim, Palaiseau

Synthetic antiferromagnets

Two **ferromagnetic** layers **antiferromagnetically** coupled through RKKY interaction

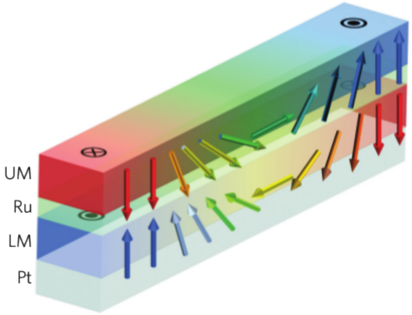

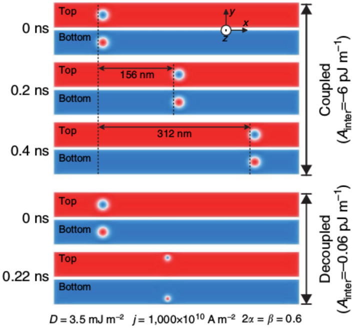

Fast current-induced domain wall motion up to 750 m s^{-1}

Compensation of the dipolar field:
→ smaller skyrmions
→ no skyrmion Hall effect

S.-H. Yang *et al.* *Nat. Nano.* 10 (2015), 221–226

X. Zhang *et al.* *Nat. Commun.* 7 (2016), 10293

Sample optimization

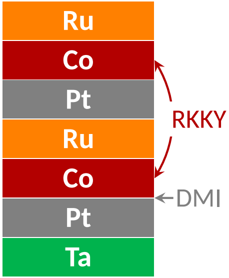

Samples from UMR CNRS/Thales
W. Legrand, F. Ajejas, Y. Sassi, V. Cros

W. Legrand *et al.* *Nat. Mater.* (2019), 1–9

Sample optimization

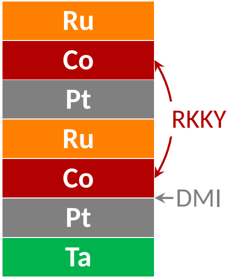

Tuning the RKKY coupling with the Ru and Pt thicknesses

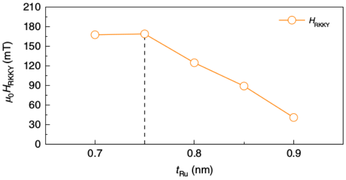

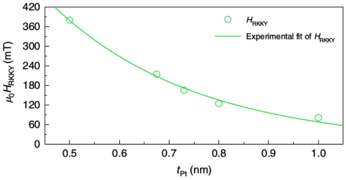

Samples from UMR CNRS/Thales
W. Legrand, F. Ajejas, Y. Sassi, V. Cros

W. Legrand *et al.* *Nat. Mater.* (2019), 1–9

Sample optimization

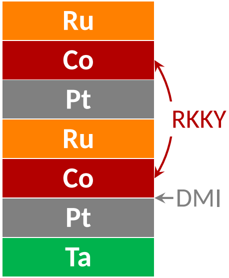

Tuning the RKKY coupling with the Ru and Pt thicknesses

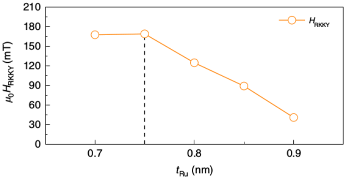

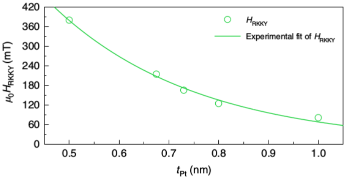

Anisotropy fixed by the Co thickness

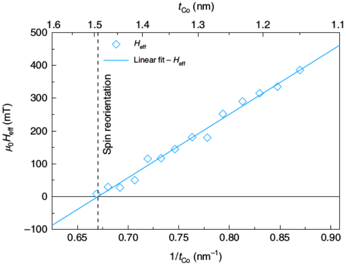

Samples from UMR CNRS/Thales
W. Legrand, F. Ajejas, Y. Sassi, V. Cros

W. Legrand *et al.* *Nat. Mater.* (2019), 1–9

Sample optimization

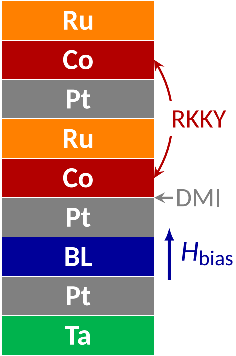

Samples from UMR CNRS/Thales
W. Legrand, F. Ajejas, Y. Sassi, V. Cros

THALES

Tuning the RKKY coupling with the Ru and Pt thicknesses

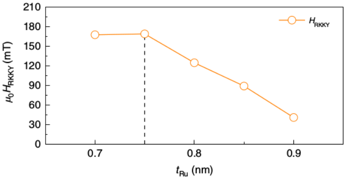

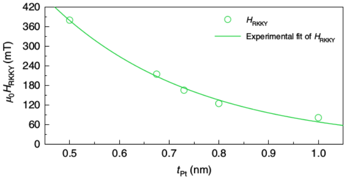

Anisotropy fixed by the Co thickness

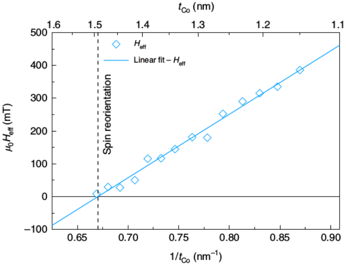

Bias field adjusted by the Pt spacer

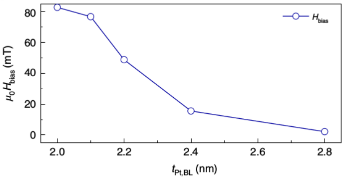

W. Legrand *et al.* *Nat. Mater.* (2019), 1–9

NV images of the non-collinear magnetic structures

Fully compensated SAF
Perpendicular anisotropy
Large out-of-plane domains

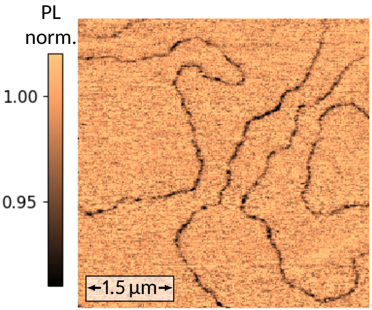

NV images of the non-collinear magnetic structures

Fully compensated SAF
Perpendicular anisotropy
Large out-of-plane domains

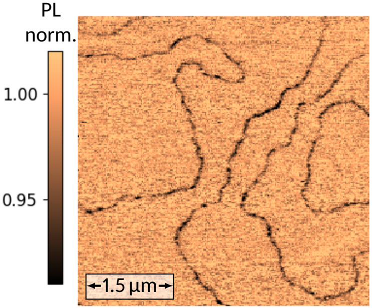

Fully compensated SAF
Vanishing anisotropy
Spin spiral

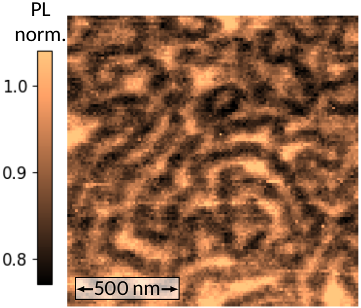

NV images of the non-collinear magnetic structures

Fully compensated SAF
Perpendicular anisotropy
Large out-of-plane domains

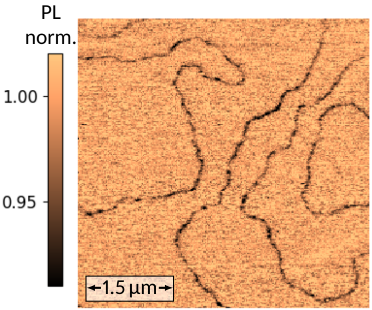

Fully compensated SAF
Vanishing anisotropy
Spin spiral

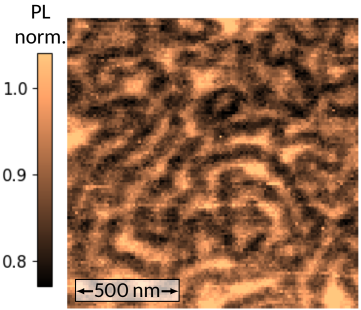

Fully compensated SAF
Biased by a FM layer
Antiferromagnetic skyrmions

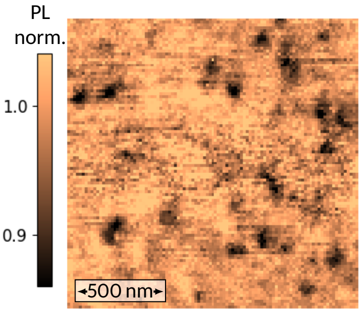

NV images of the non-collinear magnetic structures

Fully compensated SAF
Perpendicular anisotropy
Large out-of-plane domains

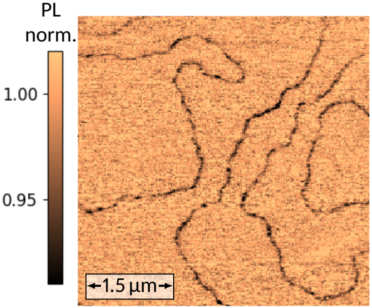

Fully compensated SAF
Vanishing anisotropy
Spin spiral

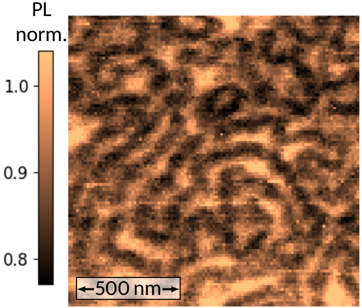

Fully compensated SAF
Biased by a FM layer
Antiferromagnetic skyrmions

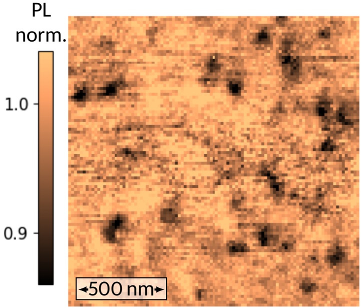

→ Are we really in high-field mode ?

Quantitative imaging of the domain walls

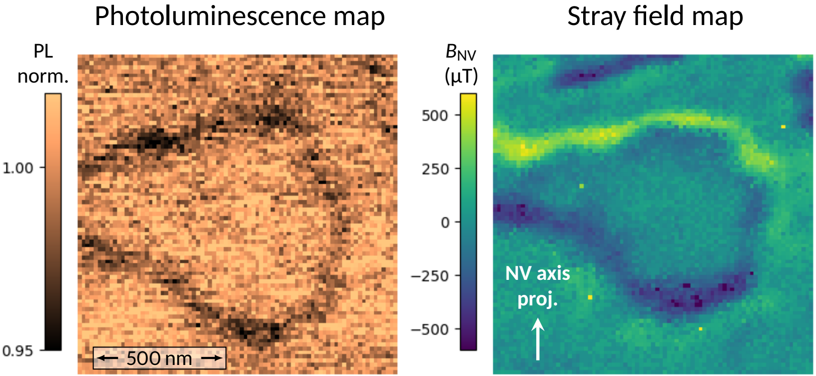

Quantitative imaging of the domain walls

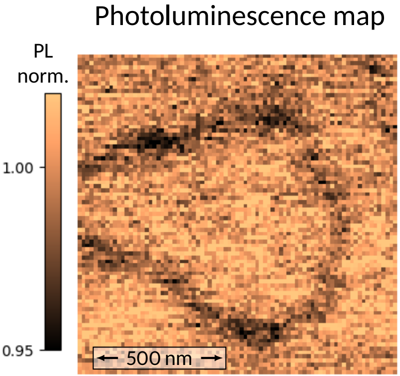

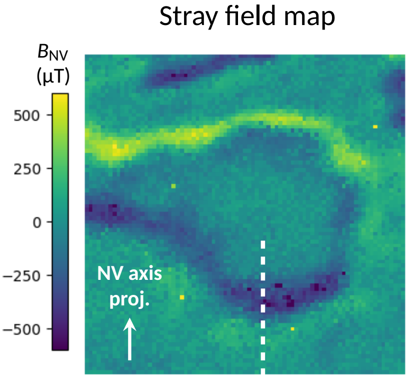

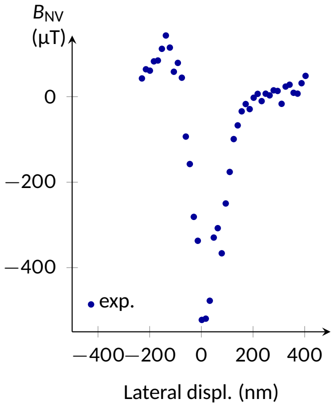

Quantitative imaging of the domain walls

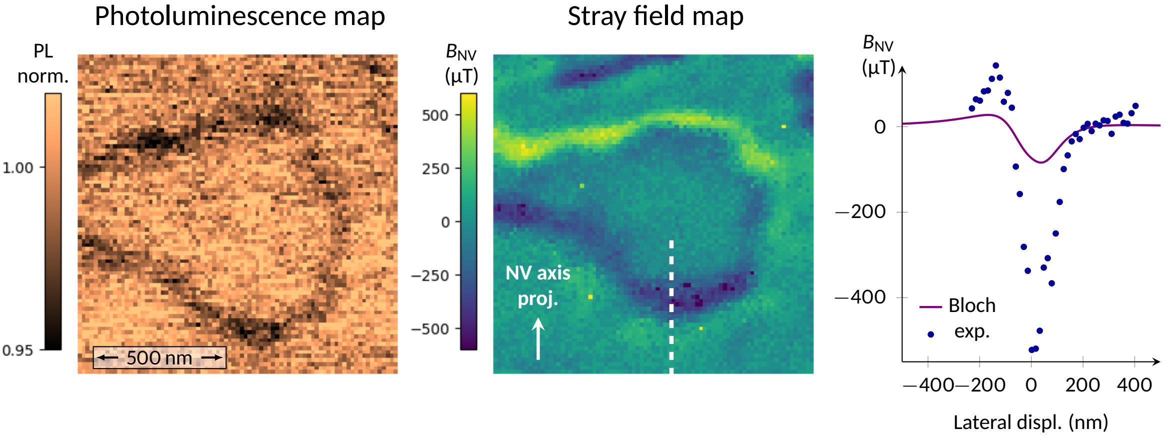

From micromagnetic calculations including the dipolar couplings:

→ Domain wall width top layer: 37 nm

→ Domain wall width bottom layer: 26 nm

Quantitative imaging of the domain walls

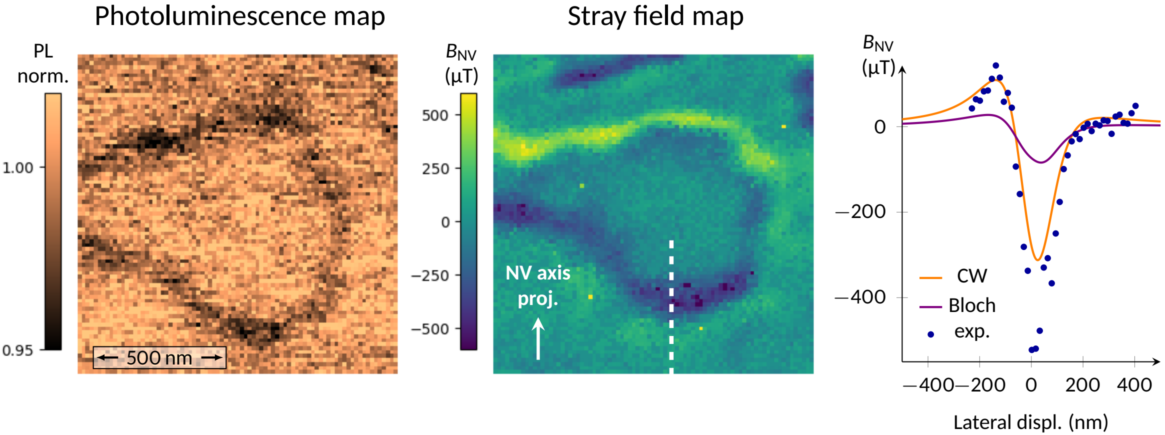

From micromagnetic calculations including the dipolar couplings:

→ Domain wall width top layer: 37 nm

→ Domain wall width bottom layer: 26 nm

Quantitative imaging of the domain walls

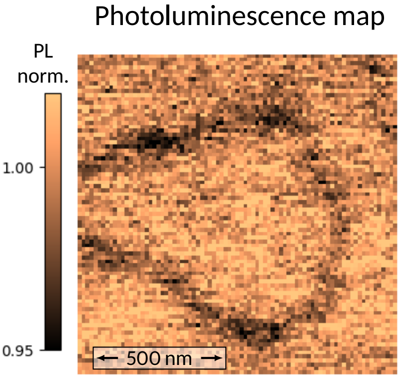

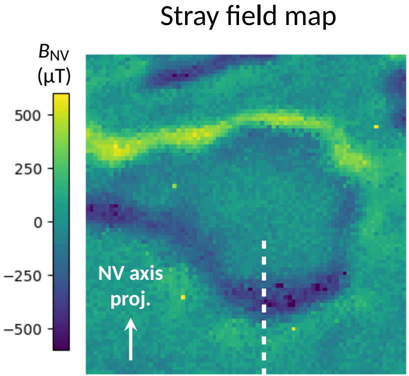

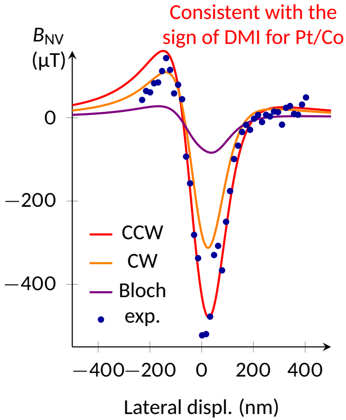

From micromagnetic calculations including the dipolar couplings:

→ Domain wall width top layer: 37 nm

→ Domain wall width bottom layer: 26 nm

Probing magnetic noise with the NV center

Detection of Johnson noise

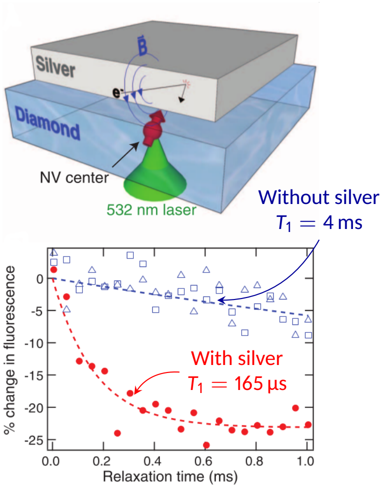

📄 S. Kolkowitz *et al.* *Science* 347 (2015), 1129–1132

Detection of ferromagnetic resonance

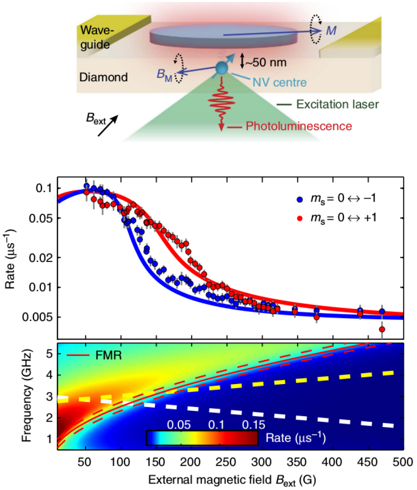

📄 T. van der Sar *et al.* *Nat. Commun.* 6 (2015), 7886

Enhancement of the spin relaxation

Optical pumping
NV spin polarized
in $m_s = 0$

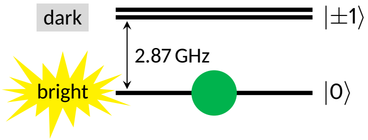

Enhancement of the spin relaxation

Optical pumping NV spin polarized in $m_s = 0$

Faster spin relaxation (smaller T_1)

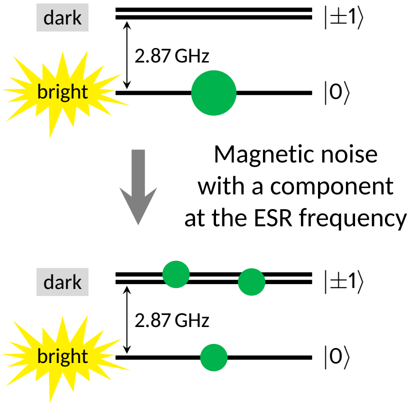

Enhancement of the spin relaxation

Optical pumping
NV spin polarized
in $m_s = 0$

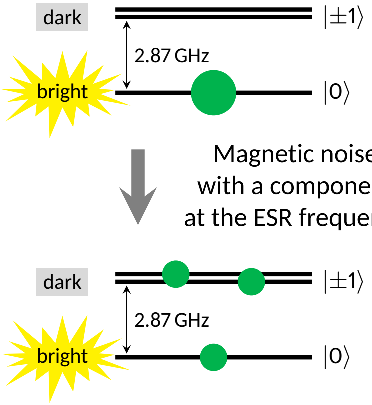

Magnetic noise
with a component
at the ESR frequency

Faster spin
relaxation
(smaller T_1)

Overall decrease of
the photoluminescence

not related to the DC $B_\perp$ field

Measurements of the spin relaxation time T_1

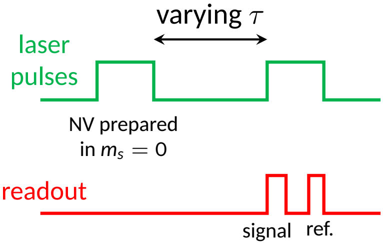

Measurements of the spin relaxation time T_1

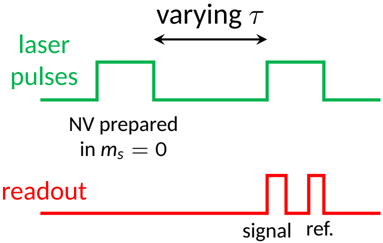

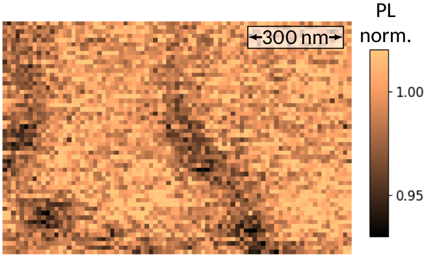

Measurements of the spin relaxation time T_1

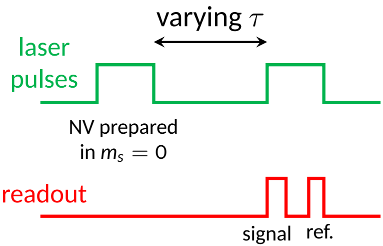

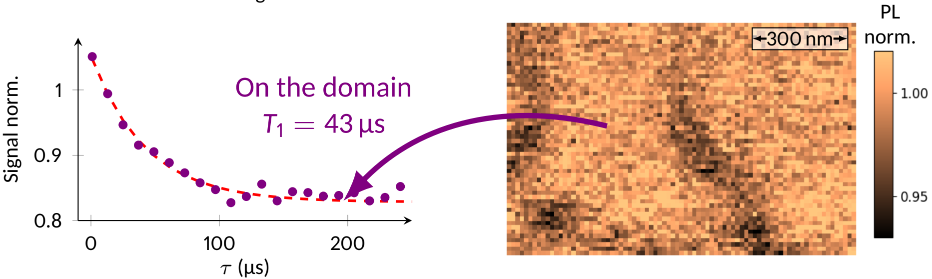

Measurements of the spin relaxation time T_1

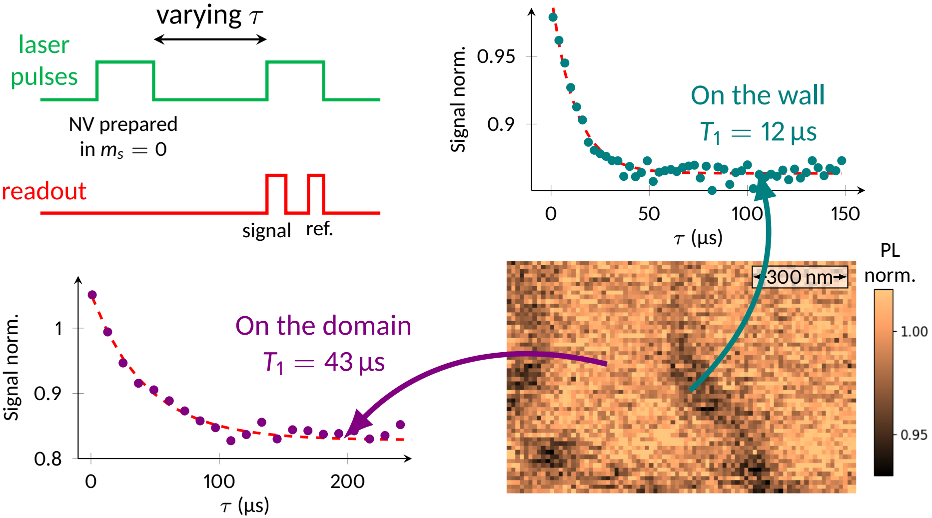

Optical power dependence

Increase of the optical power
→ More efficient polarization of the NV in the bright $m_s = 0$ state
→ Effect of the spin relaxation enhancement less visible

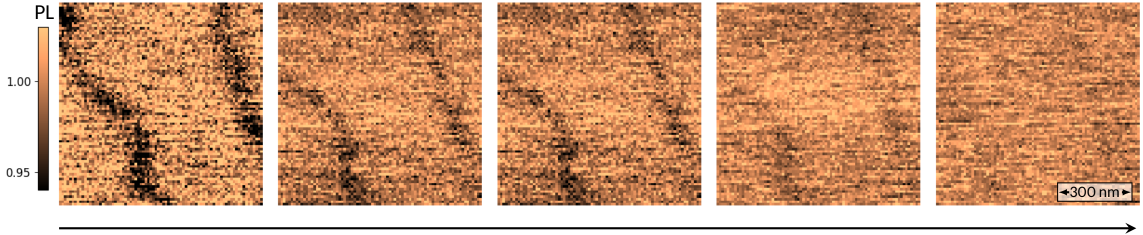

23.5 µW	50.5 µW	80.7 µW	143 µW	220 µW
$P/P_{sat} \sim 0.04$	$P/P_{sat} \sim 0.1$	$P/P_{sat} \sim 0.15$	$P/P_{sat} \sim 0.28$	$P/P_{sat} \sim 0.42$

Stronger contrast for low optical power!

Magnon dispersion

Simulation parameters:

- $M_s = 1.1\,\mathrm{MA\,m^{-1}}$
- $A = 10\,\mathrm{pJ\,m^{-1}}$
- $K = 0.8\,\mathrm{MJ\,m^{-3}}$
- $D = 0.5\,\mathrm{mJ\,m^{-2}}$
- $A_{\mathrm{RKKY}} = 0.19\,\mathrm{mJ\,m^{-2}}$

In the domains

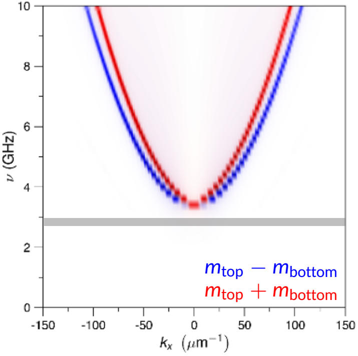

We probe inside the gap!

In the domain walls

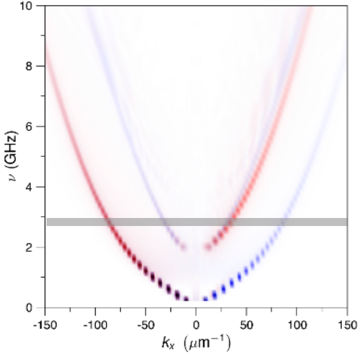

We can probe thermally activated magnons!

Calculations by J.-V. Kim

Summary

With a scanning NV-magnetometer, you can:

Study ferromagnets **at zero field** in “quenching” mode

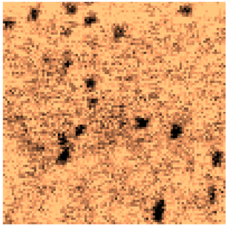

Stabilization of zero-field skyrmions in exchanged-bias layers

Investigate **antiferromagnets** in quantitative mode

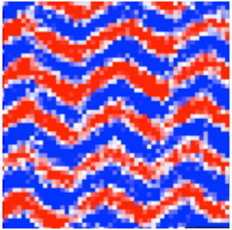

Exploration of the strain-dependent phase diagram of $BiFeO_3$ in real-space

Detect magnetic structures **using their excitation spectrum**

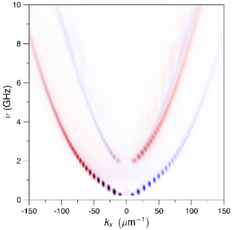

New imaging mode based on magnetic noise

Acknowledgments

L2C, Montpellier

Angela Haykal
Rana Tanos
Saddem Chouaieb
Florentin Fabre
Waseem Akhtar
Vincent Jacques

Spintec, Grenoble

Gaurav Rana
Olivier Boulle
Liliana Buda-Prejbeanu

UMR CNRS/Thales, Palaiseau

Johanna Fischer
Cécile Carrétéro
Manuel Bibes
Stéphane Fusil
Vincent Garcia

CEA, Saclay

Jean-Yves Chauleau
Théophile Chirac
Michel Viret

Synchrotron Soleil

Nicolas Jaouen

C2N, Palaiseau

Joo-Von Kim

UMR CNRS/Thales, Palaiseau

William Legrand
Fernando Ajejas
Yannis Sassi
Karim Bouzehouane
Nicolas Reyren
Vincent Cros

European Research Council
Established by the European Commission

DARPA
DEFENSE ADVANCED RESEARCH PROJECTS AGENCY

ANR
AGENCE NATIONALE DE LA RECHERCHE